Received: August 18, 2023. Revised: September 8, 2023. 482

International Journal of
Intelligent Engineering & Systems

http://www.inass.org/

Optimal Integration of Photovoltaic Public Charging Stations in Multi-Consumer Electrical Distribution System Using Improved Honey Badger Algorithm

Srinivasarao Thumati[1]* **S Vadivel[2]** **M Venu Gopala Rao[3]**

[1]*Department of Electrical Engineering, Faculty of Engineering and Technology, Annamalai University, Annamalai nagar – 608002, Tamil Nadu, India*
[2]*Government Polytechnic College, Keelapalur, Ariyalur-621707, Tamil Nadu, India*
[3]*QIS College of Engineering and Technology, Ongole-523272, Andhra Pradesh, India*
* Corresponding author's Email: srinuthumati@gmail.com

Abstract: The penetration of electric vehicle (EV) loads in the electrical distribution system (EDS) is anticipated to increase dramatically over the next few years in response to rising global warming and fuel price scenarios. Planning for charging infrastructure and renewable energy sources (RES) is urgently required in this context. By carefully combining public charging stations (PCSs) backed by photovoltaic (PVs) systems and distribution static compensators (DSTATCOMs), this study proposes an optimisation strategy to reduce the adverse effects of EV load penetration in EDS. The proposed multi-objective function aims to reduce the voltage deviation index and distribution losses while considering various operational constraints. By combining the voltage stability index (VSI) and opposition-based learning (OBL) strategy with honey badger algorithm (HBA), the optimisation problem is resolved with a smaller search space for global minima. The effectiveness of the proposed technique on IEEE 33-bus EDS was evaluated in various situations. The real power losses are reduced to 242.35 kW, 75.32 kW and 41.76 kW from 350.25 kW by optimally integrating (i) PCSs alone, (ii) simultaneous PCSs and PVs and (iii) simultaneous PCSs, PVs and DSTATCOMs, respectively. Further, the VSI of the EDS is enhanced 0.7057, 0.8727, 0.9018 from 0.6104, respectively. The computational characteristics of HBA were also measured and compared with those of the COA and HBA. In terms of target and computational time, the outcomes produced by IHBA are very competitive with those of COA and superior to those of HBA. Additionally, even with a high EV load penetration, the suggested methodology produces reduced distribution losses and an appropriate voltage profile in EDS.

Keywords: Electrical distribution system, Electric vehicles, Photovoltaic system, Distribution static compensator, IHBA optimizer, Voltage stability index, Opposition-based learning.

1. Introduction

The international energy agency (IEA) has warned that transportation contributes to one-third of end-use CO_2 emissions, with global transport-related emissions expected to rise by 3-8 billion metric tons by 2022. On the other side, the energy sector is responsible for 73% of the global greenhouse gas (GHG) emissions [1]. To reduce emissions, urgent actions from the transportation and energy sectors are needed, including the integration of renewable energy sources (REs) and adoption of electric vehicles (EVs). Wind and solar power generation is expected to exceed electricity demand by 2023. However, managing potential challenges such as the impact of EVs on electrical systems is crucial for a successful low-carbon shift [2].

Due to the intermittent nature of REs and the stochastic nature of EVs, optimization of EDS's performance focuses primarily on loss reduction, voltage profile, voltage stability enhancement, loadability improvement, reliability improvement, and power quality issues mitigation—has recently gained popularity as a research area. For these two technologies to achieve their intended benefits, coordinated planning in EDS is essential [3].

The improvement of the electric distribution system (EDS) performance is covered in the literature using a variety of techniques. It is highly advised to allocate renewable energy (RE) based distribution generation (DG) efficiently, and a number of heuristic algorithms have been used to address this difficulty, as shown in references [4–8]. To obtain the best placement of REs, distribution-static synchronous compensators (D-STATCOM), and passive power filters (PPFs) within the EDS framework, reference [5] uses the artificial rabbit optimiser (ARO). The goal of this optimisation is to improve the power quality and performance. The ideal locations and sizes of various types of DGs were determined in [6] using a novel method employing the improved decomposition-based evolutionary algorithm (I-DBEA). The multi-objective function addressed by this method includes elements such as the power loss, voltage variation, and voltage stability. Similarly, [7] addressed the DG allocation problem in single- and multi-objective scenarios using the transient search optimisation (TSO) approach. It considers variables such as the voltage stability, voltage variation, and power loss. To address a variety of DG types and account for load increase, [8] suggested a novel method that combines weight-improved particle swarm optimisation (WIPSO) and gravitational search algorithm (GSA). These findings show that the strategic integration of RE-based DGs significantly improves the EDS performance. It is crucial to realize that these works do not address the difficulties caused by the emerging EV load trends in the electric sector, including their possible negative effects on EDS's performance.

EV load penetration and EV charging stations have been considered for solving the optimal allocation of REs problems in several publications [9–13]. The honey badger algorithm (HBA) was used in [9] to determine the best placement and size for photovoltaic systems (PV) to reduce the detrimental effects of high EV load penetration in the EDS. Particle swarm optimisation (PSO) and butterfly optimisation (BOA) were used in [10] to define and solve a weighted-sum multi-objective function that considers the network's EV fast-charging stations (FCSs) and distribution losses. However, these studies have not been optimised for FCS placement. To properly limit the effects of EV load penetration, the coyote optimisation algorithm (COA) was modified in [11] for the optimal integration of PV-based DG into a multi-feeder distribution system. It also emphasises the necessity of battery energy storage systems (BESS) for dealing with islanding circumstances. In [12], various DG types were combined optimally using PSO while considering the EV impact in the form of either a vehicle-to-grid (V2G) or grid-to-vehicle (G2V) mode. [13] used demand response (DR) and smart charging/discharging of EV CSs to simultaneously focus on reliability enhancement, loss reduction, and voltage profile optimisation. Based on these investigations, it is possible to enhance EDS's functionality of EDS by precisely positioning or managing the EV CS. However, these studies did not address the combined effects of RE.

However, several studies [14–18] concentrated on the best integration of EV charging stations (EV-CSs). A balanced mayfly algorithm (BMA) was created in [14] to design and place EV-CSs in EDS in the best possible manner while taking loss reduction and operational cost into account. In [15], the issue of the best integration of EV CSs was resolved by considering various EV CS types and their charging rates, with an emphasis on loss, voltage profile, and investment and operating costs. In [16], the non-dominated sorting genetic algorithm II (NSGA-II) with a Fuzzy set is used to correlate the distribution loss and EV CS usage factor to optimally integrate EV CSs. To optimally integrate capacitor banks (CBs) for reactive power control in the presence of a fluctuating EV load, advanced grey wolf optimiser-particle swarm optimisation (AGWO-PSO) was proposed in [17]. The improvement of the EDS performance and reliability while considering the V2G and G2V scenarios is the focus of this study. In [18], hybrid grey wolf optimiser-particle swarm optimisation (GWO-PSO) was employed to address EV CS integration while lowering land and installation costs, as well as distribution losses. Notably, our studies have demonstrated how effectively integrating EVs into EDS while using intelligent charging and discharging scenarios may also significantly boost network performance. However, they do not work concurrently with the EV effect mitigation and RE-based DGs.

However, some recent efforts [19–23] have also concentrated on the concurrent optimal integration of REs and EV charging stations (EV-CSs). In [19], the multi-objective red kite optimisation algorithm (MOROA) was used to simultaneously solve the optimal integration of REs and EV fast-charging stations (FCSs) while reducing loss and improving the voltage profile. In [20], a hybrid PSO-GA was developed and used to reduce the loss and voltage deviation while optimally integrating PVs with EV-CSs. It uses PSO and a genetic algorithm (GA).

When determining the best sites and sizes for PV, WTs, and EV-CSs in [21], numerous reliability indices were optimised while considering India's

Table 1. Comparison of literature and proposed methodology based on allocation problem

References	Type of allocation problem				
	Only REs allocation	Only REs allocation with EV penetration	Only CSs allocation	Simultaneous allocation of REs + CSs	Simultaneous allocation of REs + CSs + DSTATCOMs
[4-8]	✓	–	–	–	–
[9-13]	–	✓	–	–	–
[14-18]	–	–	✓	–	–
[19-23]	–	–	–	✓	–
Proposed	✓	✓	✓	✓	✓

weather patterns and EV demand increase into account. In [22], Harris hawks optimisation (HHO) was used to optimise the loss, voltage profile, placement based on EV density, and cost of the EV CS investment. The placement and dimensions of PV-based DGs were integrated to offset the demand for the EV CS load simultaneously. In [23], the performance of EDS was maximised by appropriately locating and sizing RE-based DGs concentrating on techno-environmental objectives using the CPLEX solver in the GAMS software. The benefits of EV CS operators are optimised in the first stage utilising the V2G and G2V scenarios.

In Table 1, the literature works are compared with the proposed methodology based on the optimal allocation problem. The performance of EDS is improved by solving for (i) only REs allocation, (ii) REs allocation considering EV load penetration, (iii) allocation of only CSs, and (iv) simultaneous allocation of both REs and CSs. The major contributions of this study are as follows.

1) A multi-objective function focusing on techno-economic-environmental objectives was formulated while solving the simultaneous allocation of PVs, public charging stations (PCSs), and DSTATCOMs.
2) The objective function is solved using an improved honey badger algorithm (IHBA) with an opposition-based learning (OBL) strategy.
3) Simulations were performed on the IEEE 33-bus test system for different EV load growth scenarios and compared with the literature.
4) For different scenarios, the optimal allocation problem is solved with IHBA and compared its performance with basic HBA and COA

The remainder of the paper is structured as follows: The mathematical modelling of relevant concepts, including voltage-dependent multi-type customer load modelling, PCS, PVs, and DSTATCOM, is explained in section 2. The equal and unequal constraints of the proposed multi-objective optimisation problem focusing on loss voltage deviation are described in section 3. The IHBA with OLB and voltage stability index (VSI) solution approaches are described in section 4. Numerous case studies on the IEEE 33-bus system are presented in section 5, utilising the suggested methodology. The overall contributions of this study are presented in detail in section 6.

2. Modelling of concepts

This section explains the mathematical modelling of the major keywords of this study, such as multi-type consumers, public charging station loads, photovoltaic systems, and distribution static compensators.

2.1 Multi-type consumer load modeling

In reality, different types of consumers are usually associated with EDS, and their loads are periodically sensitive to changes in the voltage profile. Thus, this study used voltage-dependent load modelling for residential, industrial, commercial, and electric vehicles.

$$\bar{P}_{ld,k} = P_{ld,k}\left(k_r V_k^{\alpha_r} + k_c V_k^{\alpha_c} + k_i V_k^{\alpha_i}\right) \quad (1)$$

$$\bar{Q}_{ld,k} = Q_{ld,k}\left(k_r V_k^{\beta_r} + k_c V_k^{\beta_c} + k_i V_k^{\beta_i}\right) \quad (2)$$

In this model, the substation bus or reference bus voltage is assumed to be constant irrespective of the load changes in the EDS.

2.2 Public charging station modeling

In specific, public charging stations (PCS) need to accommodate multiple vehicles for charging at a time. Thus, number of charging ports (CPs) and their power ratings define the total load demand of PCS, and it is given by;

$$P_{pcs,k} = n_{cp,l1} \times P_{ev,l1} + n_{cp,l2} \times P_{ev,l2} \quad (3)$$

$$Q_{pcs,k} = P_{pcs,k} \times tan(cos^{-1}\varphi_{cs}) \quad (4)$$

$$\bar{P}_{ld,k} = P_{ld,k} + P_{pcs,k} \times (1 + \rho_{ev}) V_k^{\alpha_{ev}} \quad (5)$$

$$\bar{Q}_{ld,k} = Q_{ld,k} + Q_{pcs,k} \times V_k^{\beta_{ev}} \quad (6)$$

$$npcs = \left(\sum_{k=1}^{nbus} \bar{P}_{ld,k}\right)/P_{pcs} \quad (7)$$

2.3 Photovoltaic system

Photovoltaic systems (PVs) usually inject real power into the grid via their associated inverters while maintaining a unity power factor. Thus, PVs can be seen as real power compensator at its integrated bus, as given by,

$$\bar{P}_{ld,k} = P_{ld,k} - P_{pv,k} \quad (8)$$

2.4 Distribution static compensator

A distribution static compensator (DSTATCOM) is used to compensate for the reactive power in the grid and thus maintain a good voltage profile. The corresponding modelling as reactive power compensation at its integrated bus, as given by,

$$\bar{Q}_{ld,k} = Q_{ld,k} - Q_{dst,k} \quad (9)$$

3. Problem formulation

By integrating the PCS, EDS can experience a low voltage profile, high distribution losses, and low voltage stability margin. Thus, the proposed multi-objective is focused on optimizing these three operating goals simultaneously.

3.1 Objective function

3.1.1. Real power distribution loss

The distribution system real power losses are dependent on current flow in each branch and their resistance, related by,

$$f_1 = P_{loss} = \sum_{k=1}^{nbr} I_k^2 r_k \quad (10)$$

3.1.2. Voltage deviation index

The voltage levels at each bus must be maintained constant without significant deviation from the low and/or high permissible limits. Thus, voltage deviation index (VDI) is given by,

$$f_2 = VDI = \frac{1}{nbus}\sum_{i=1}^{nbus} |V_r - V_i|^2 \quad (11)$$

3.1.3. Overall objective function

The overall objective function minimises both individual objective functions simultaneously, and is given by,

$$OF = min(f_1 + f_2) \quad (12)$$

3.2 Constraints

The objective functions defined in Eq. (12) is constrained by the following equal and unequal constraints, which must be addressed in the optimisation process.

$$I_k \leq I_{k,max} \quad (13)$$

$$V_{i,min} \leq V_i \leq V_{i,max} \quad (14)$$

$$\sum_{i=1}^{npv} P_{pv,i} \leq \sum_{i=1}^{nbus} P_{ld,i} + \sum_{k=1}^{npcs} P_{pcs,k} \quad (15)$$

$$\sum_{i=1}^{ndst} Q_{dst,i} \leq \sum_{i=1}^{nbus} Q_{ld,i} + \sum_{k=1}^{npcs} Q_{pcs,k} \quad (16)$$

4. Solution methodology

The solution methodology in this study was developed using a hybrid approach with a recent improved variant of honey badger algorithm (IHBA) with opposition based learning (OBL) and the voltage stability index (VSI). In the first stage, the search space in the optimisation process using IHBA is reduced by determining predefined candidate locations using VSI, and the sizes of PVs and DSTATCOMs are optimally tuned using IHBA. This section explains the mathematical concepts of IHBA and VSI and their application in solving the proposed multi-objective function.

4.1 Honey badger algorithm

Hashim et al. [24] developed the honey badger algorithm (HBA), like a general optimisation strategy by incorporating both the exploration and exploitation stages. The HBA stages are mathematically defined as follows: HBA begins by generating an initial population of *N* solutions (honey badgers) using Eq. (17).

$$h_{pq} = L_{pq} + r_1 \times \left(U_{pq} - L_{pq}\right) \quad (17)$$

where $p = 1, \ldots, n$ and $q = 1, \ldots, d$, U_{pq} and L_{pq} are the minimum and maximum limits of the variables of optimization problem, respectively; r_1 is a randomised factor between 0 and 1, h_{pq} is the location of *p*th honey badger in *q*th solution vector, *n* and *d* are the size of population and their dimensions, respectively.

The next stages of HBA are termed as digging and honey as similar to exploration and exploitation phases in regular meta-heuristic algorithms.

In *digging phase* (exploration), honey badger location is updated using smell intensity and changes in flying direction, as given by,

$$h_{pq}^{k+1} = h_{pq}^{b,k} + f_d \times \gamma \times s_i \times h_{pq}^{b,k} + f_d \times r_2 \times \delta \times d_p \times |cos(2\pi r_3) \times [1 - cos(2\pi r_4)]| \quad (18)$$

where h_{pq}^{k+1} is the new position of honey badger, r_2, r_3 and r_4 are the random numbers, d_p is the distance of pth honey badger with best prey at *k*th iteration, $h_{pq}^{b,k}$, $\gamma \geq 1$ and to define the ability of honey badger to explore the food and is set to 6, δ is a dynamic decreasing factor to tune exploration to exploitation, s_i and f_d are the smell intensity and changes in flying direction, respectively. Mathematically,

$$s_i = r_5 \times \frac{C}{4\pi d_p^2} \quad (19)$$

$$f_d = \begin{cases} +1 & if\ r_6 \leq 0 \\ -1 & other\ wise \end{cases} \quad (20)$$

$$\delta = \tau \times e^{(k/K)}, \tau > 1 \quad (21)$$

where $C = \left(h_{pq}^{k} - h_{pq}^{k+1}\right)^2$ is the prey strength of concentration and $d_p = \left(h_{pq}^{b,k} - h_{pq}^{k}\right)$ is the distance between best prey and present honey badger, respectively, r_5 and r_6 are the random numbers, k and K are the number to represent present and maximum iteration, respectively; τ is a constant equal to 2.

In the *honey phase* (exploitation), the follower behaviour of honey badger to arrive a beehive by following a guide honey badger. Mathematically, this situation is formulated as,

$$h_{pq}^{k+1} = h_{pq}^{b,k} + f_d \times r_7 \times \delta \times d_p \quad (22)$$

Based on spatial search information of d_p, Eq. (22) helps to surrounds nearly to best prey $h_{pq}^{b,k}$. At this stage, the direction of search is influenced by dynamic behaviour δ and f_d.

4.2 Opposition-based learning

This paper improves the HBA algorithm by maintaining population diversity during the search process, resulting in better convergence towards the global optima. The proposed improved HBA (IHBA) uses the opposition-based learning (OBL) strategy to preserve candidate solutions' diversity and improve convergence [25], ensuring efficient searching of the entire search space. The OBL strategy calculates a solution in the opposite direction of a candidate solution to explore more promising regions.

$$\bar{h}_{pq} = U_{pq} + L_{pq} - h_{pq} \quad (23)$$

where $\bar{h}_{pq}$ is a population located in the opposite direction.

4.3 Voltage stability index

Further to OBL, voltage stability index (VSI) based candidate locations are determined to limit the search space in this paper.

$$VSI_j = V_i^4 - 4\left(x_{ij}P_j - r_{ij}Q_j\right)^2 - 4\left(r_{ij}P_j + x_{ij}Q_j\right)V_i^2, \quad VSI_j \geq 0, j = 2{:}nbus \quad (24)$$

In the stability concept, $VSI_j \geq 0$ ensures reliable functioning [26]. Once load flow has been completed, the VSI of each bus will be determined and rated in ascending order. Because the top-ranked places are more reliable for instable, they are the areas where PV systems and DSTACOMs should be integrated, respectively. The least stable sites, on the other hand, are very stable and are employed as the search space to integrate PCSs. By doing this, the search space is diversified to provide effective, reliable, and long-lasting networks.

5. Results and discussion

Simulation results are performed on IEEE 33-bus test system for different case studies. The following are the major assumptions of this paper. In each PCS, there are 30 ($n_{cp,l1}$) and 20 ($n_{cp,l2}$) charging ports for level-1 and level-2 charging, respectively. The power ratings of level-1 and level-2 chargers are assumed to be 11 kW ($P_{ev,l1}$) and 22 kW ($P_{ev,l2}$), respectively. Thus, the total power demand of PCS is $P_{pcs,k}$ =770 kW (i.e., 30×11 + 20×22) with an operating power factor $cos(\varphi_{cs})$ of 0.95 lagging. The voltage-dependent load modelling power coefficients are taken from (α_r, α_c and α_i) and (β_r, β_c and β_i) [27]. The load scaling factors at each bus for different types of loads are considered as k_r=0.5, k_c=0.3 and k_i =0.2.

In each system, the total EV load penetration is assumed to be ρ_{ev}=50% to the total base case load of the system. Simulations are carried out for the following scenarios: (i) optimal integration of PCSs alone, (ii) optimal sizing of PVs at each PCS, and (iii) simultaneously optimal sizing of PVs and DSTATCOMs at each PCS, respectively. Each scenario is repeated using IHBA, COA and HBA.

The computational features of these algorithms are quantified based on 50 independent trails of each case. The number of iterations for all algorithms is 50. The simulation results of all case studies and comparisons are presented in Table 2.

The base system with three types of consumers at each bus has real and reactive power loads of 3558.408 kW and 2091.561 kVAr, respectively. The system is suffering by real and reactive power losses of 163.99 kW and 108.824 kVAr, respectively. Further, the lowest voltage magnitude of 0.9212 p.u is registered at bus-18 and overall VSI is determined equal to 0.7204, respectively. This operating state is treated as Case 0.

By considering $\rho_{ev} = 50\%$ extra EV load penetration, the network performance is evaluated. The real and reactive power loads of the system are increased to 5057.833 kW and 3320.903 kVAr, respectively. The real and reactive power losses are increased to 350.2476 kW and 231.8228 kVAr, respectively. Further, the lowest voltage magnitude of 0.8839 p.u is registered at bus-18 and overall VSI is determined equal to 0.6104, respectively. This operating state is treated as case 1.

From case 0, it can be seen that the losses are increased significantly and voltage profile and VSI are decreased drastically due to EV load penetration.

5.1 Optimal allocation of PCSs

In comparison to Case 0, the real power load due to 50% of EV penetration is increased by 1489.785 kW. As per the designed capacity of 770 kW, only two PCSs are sufficient to meet this load. However, by considering ¼ of the day as non-working time of PCS, and 15% overlapping scenario, the number charging stations are determined as 3. The optimal locations for integrating PCSs are determined by IHBA as buses 2, 19 and 25.

The real and reactive power loads of the system are increased to 5720.331 kW and 4147.856 kVAr, respectively. The real and reactive power losses are increased to 252.3468 kW and 157.7249 kVAr, respectively. Further, the lowest voltage magnitude of 0.9165 p.u. is registered at bus-18 and overall VSI is determined equal to 0.7057, respectively. This operating state is treated as case 2.

In comparison to case 1, though the EV load is more in case 2, but the losses are decreased potentially and voltage profile and VSI are improved significantly due to optimal integration of PCSs, respectively.

5.2 Optimal allocation of PVs in EDS with optimal PCSs

In this case 3, it aimed to improve the performance of EDS with optimal PCSs by optimally integrating PVs. The best locations and sizes of PVs are determined by IHBA are buses 13, 25 and 30 and the corresponding sizes are 562 kW, 1589 kW, and 1286 kW, respectively. By this, the net real and reactive power loadings on the system are decreased to 2538.31 kW and 4011.962 kVAr, respectively. The real and reactive power losses are decreased to 75.317 kW and 50.849 kVAr, respectively. Further, the lowest voltage magnitude of 0.9665 p.u is registered at bus-18 and overall VSI is determined equal to 0.8727, respectively.

In comparison to case 1 and case 2, in this case 3, the losses are decreased significantly and voltage profile and VSI are improved effectively due to optimal integration of PVs, respectively.

5.3 Optimal allocation of PVs, DSTATCOMs and PCSs

In this case 4, it aimed to improve the performance of EDS with optimal PCSs and PVs by optimally integrating DSTATCOMs. The best locations and sizes of DSTATCOMs are determined by IHBA are buses 2, 7 and 24 and the corresponding sizes are 2045.936 kVAr, 739.333 kVAr, and 1556.122 kVAr, respectively. By this, the net real and reactive power loadings on the system are decreased to 2550.96 kW and 1450.141 kVAr, respectively. The real and reactive power losses are decreased to 41.763 kW and 30.181 kVAr, respectively. Further, the lowest voltage magnitude of 0.9745 p.u is registered at bus-18 and overall VSI is determined equal to 0.9018, respectively.

In comparison to case 1, case 2 and case 3, in this case 4, the losses are decreased significantly and voltage profile and VSI are improved effectively due to simultaneous optimal integration of PCSs, PVs and DSTATCOMs, respectively. The comparison of all these case studies is given in Table 2. Further, the voltage profile of the system is compared in Fig. 1.

5.4 Comparative study

A comparative study was conducted in Table 3 using standard IEEE 33-bus test system data with constant power load modelling. The actual loading of the test system without EV load penetration was 3715 kW and 2300 kVAr. The losses were 202.667 kW and 134.896 kV Ar, respectively. The lowest voltage was

Table 2. Comparison of system performance for different case studies

Case #	P_{load} (kW)	Q_{load} (kW)	P_{loss} (kW)	Q_{loss} (kW)	V_{min} in p.u. (bus #)	VSI
0	3558.05	2091.56	163.99	108.82	0.9213 (18)	0.7204
1	5047.83	3320.90	350.25	231.82	0.8839 (18)	0.6104
2	5720.33	4147.86	242.35	157.72	0.9165 (18)	0.7057
3	2538.31	4011.96	75.32	50.85	0.9665 (18)	0.8727
4	2550.96	1450.14	41.76	30.18	0.9745 (18)	0.9018

Table 3. Comparison of IHBA with literature works and other algorithms

Ref/ Method	PV in kW (bus #)	P_{loss} (kW)					Time (s)
		Best	Worst	Mean	Median	SD	
Base	–	–	–	–	–	–	–
ARO [5]	759 (14), 1076 (24), 1069 (30)	71.464	75.303	72.450	72.255	0.810	18.541
I-DBEA [6]	1098 (13), 1097 (24), 1715 (30)	94.8514	–	–	–	–	–
TSO [7]	772 (14), 1104 (24), 1065 (30)	72.79	–	–	–	–	–
WIPSO-GSA [8]	755 (14), 1100 (24), 1072 (30)	71.3	–	–	–	–	–
COA	757(14), 1087 (24), 1084 (30)	70.517	76.882	71.341	71.170	1.625	18.562
HBA	1094 (30), 749 (14), 1087 (24)	70.521	94.409	72.731	71.170	4.717	18.673
IHBA	1086 (24), 756 (14), 1085 (30)	70.517	79.710	71.689	70.825	2.324	18.426

Table 4. Comparison of system performance with optimal PV systems

Case #	P_{load} (kW)	Q_{load} (kW)	P_{loss} (kW)	Q_{loss} (kW)	V_{min} in p.u. (bus #)	VSI
Base	3715	2300	202.667	134.896	0.9132 (18)	0.6953
COA	3715	2300	70.517	48.79	0.9698 (33)	0.8845
HBA	3715	2300	70.521	48.801	0.97 (33)	0.884
IHBA	3715	2300	70.517	48.78	0.9698 (33)	0.8852

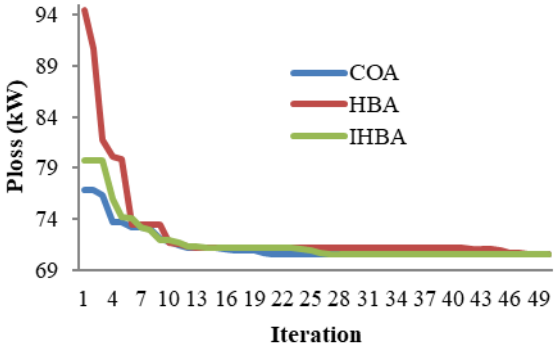

Figure. 1 Comparison of voltage profile for different case studies

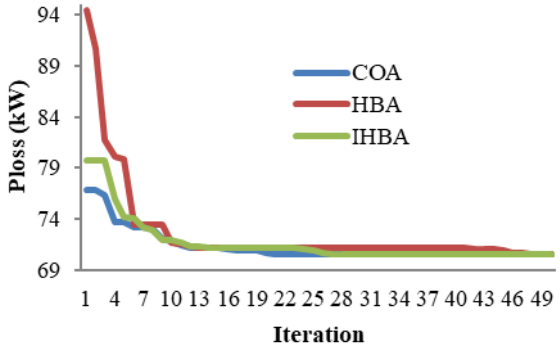

Figure. 2 Convergence characteristics of compared algorithms for best case

0.9132 p.u. on bus -18 and the overall VSI was 0.6953. Considering loss reduction as a major objective function, three PV DGs units were optimally integrated in this comparative study.

At the best locations (buses 14, 24, and 30) and corresponding optimal sizes (1086, 756, and 1085 kW), the losses are reduced to 70.517 kW. Compared to ARO [5], I-DBEA [6], TSO [7], and WIPSO-GSA [8], the proposed IHBA provides better results. In addition, the COA becomes highly competitive with the best objective function.

However, the mean, median, and standard deviation (SD) over 50 independent runs of the IHBA were better than those of the basic HBA and COA. In addition, the average computational time was low for the IHBA. The network performance in terms of active and reactive power losses, voltage profile and VSI is given in Table 4. In this regard, the combined approach of HBA with OBL and VSI outperformed the literature and compared works.

6. Conclusion

This paper proposes optimal integration of PVs, PCSs and DSTATCOMs for balancing both active and reactive power loads in the EDS and thus, the

overall performance proposed to optimize by reducing losses and voltage profile. The multi-objective function is solved using IHBA and compared its performance with basic HBA and COA. The real power losses are reduced to 242.35 kW, 75.32 kW and 41.76 kW from 350.25 kW by optimally integrating (i) PCSs alone, (ii) simultaneous PCSs and PVs and (iii) simultaneous PCSs, PVs and DSTATCOMs, respectively. Further, the VSI of the EDS is enhanced 0.7057, 0.8727, 0.9018 from 0.6104, respectively. In addition, IHBA has outperformed than literature and basic HBA and COA in terms of global optima and computational time.

Notations

$P_{ld,k}$	Nominal real power ratings of bus-*k*,
$Q_{ld,k}$	Nominal reactive power ratings of bus-*k*,
$\bar{P}_{ld,k}$	Net real power ratings of bus after modifications
$\bar{Q}_{ld,k}$	Net reactive power ratings of bus-*k* after modifications
k_r, k_c, & k_i	Load scaling factors to represent residential, commercial and industrial type of loads at bus-*k*, respectively
α_r, α_c & α_i	Coefficients of real power loads as per the voltage-dependent load modelling, respectively
β_r, β_c & β_i	Coefficients of reactive power loads as per the voltage-dependent load modelling, respectively
V_k	Voltage magnitude of bus-*k*
$V_{i,min}$	Minimum voltage limit
$V_{i,max}$	Maximum voltage limit
$P_{pcs,k}$	Total real power load demands of a PCS at bus-*k*
$Q_{pcs,k}$	Total reactive power load demands of a PCS at bus-*k*
$cos(\varphi_{cs})$	Operating power factor of the AC/DC converter at PCS
$n_{cp,l1}$	Number of level-1 charging ports in a PCS
$n_{cp,l2}$	Number of level-2 charging ports in a PCS
$P_{ev,l1}$	Power ratings of level-1 charging ports
$P_{ev,l2}$	Power ratings of level-2 charging ports
α_{ev} & β_{ev}	Coefficients of EV's real and reactive power loads as per the voltage-dependent load modelling
ρ_{ev}	EV load growth scenario
$nbus$	Number of buses in EDS.
nbr	Number of branches in the EDS
npv	Number of PVs
$ndst$	Number of DSTATCOMs
$npcs$	Number of PCSs
$P_{pv,k}$	Real power injection by PV system at bus-*k*.
$Q_{ds,k}$	Reactive power injection by DSTATCOM at bus-*k*.
P_{loss}	Total distribution real power loss
I_k	Current flow through branch-*k*
$I_{k,max}$	Maximum current flow limit for branch-*k*
r_k=r_{ij}	Resistance of branch-*k* connected between buses *i* and *j*
$x_k = x_{ij}$	Reactance of branch-*k* connected between buses *i* and *j*
VDI	Voltage deviation index
V_r	Voltage magnitude of reference or substation bus
OF	Overall objective function
f_1	Objective function 1 for real power loss
f_2	Objective function 2 for voltage deviation
VSI_j	Voltage stability index of bus-*j*,
P_j	Real power load of bus-*j*,
Q_j	Reactive power load of bus-*j*,

Conflicts of interest

The authors declare no conflict of interest.

Author contributions

Conceptualization, methodology, software and original draft preparation are done by Srinivasarao Thumati; supervision, review, and formal analysis are done by Vadivel V and Venu Gopala Rao M.

References

[1] https://www.iea.org/reports/transport-energy-and-co2

[2] H. S. Das, M. M. Rahman, S. Li, and C. W. Tan, "Electric vehicles standards, charging infrastructure, and impact on grid integration: A technological review", *Renewable and Sustainable Energy Reviews*, Vol. 120, p. 109618, 2020.

[3] A. Alsharif, C. W. Tan, R. Ayop, A. Dobi, and K. Y. Lau, "A comprehensive review of energy management strategy in Vehicle-to-Grid technology integrated with renewable energy sources", *Sustainable Energy Technologies and Assessments*, Vol. 47, p. 101439, 2021.

[4] M. Kumar, A. M. Soomro, W. Uddin, and L. Kumar, "Optimal multi-objective placement and sizing of distributed generation in distribution system: a comprehensive review", *Energies*, Vol. 15, No. 21, p. 7850, 2022.

[5] R. R. Chegudi, B. Ramadoss, and R. R. Alla, "Simultaneous allocation of renewable energy sources and custom power quality devices in electrical distribution networks using artificial rabbits optimization", *Clean Energy*, Vol. 7, No. 4, pp. 795-807, 2023.

[6] A. Ali, M. U. Keerio, and J. A. Laghari, "Optimal site and size of distributed generation allocation in radial distribution network using multi-objective optimization", *Journal of Modern Power Systems and Clean Energy*, Vol. 9, No. 2, pp. 404-415, 2020.

[7] J. S. Bhadoriya and A. R. Gupta, "A novel transient search optimization for optimal allocation of multiple distributed generator in the radial electrical distribution network", *International Journal of Emerging Electric Power Systems*, Vol. 23, No. 1, pp. 23-45, 2021.

[8] A. Rajendran and K. Narayanan, "Optimal installation of different DG types in radial distribution system considering load growth", *Electric Power Components and Systems*, Vol. 45, No. 7, pp. 739-751, 2017.

[9] S. Thumati, S. Vadivel, and M. Rao, "Honey badger algorithm based network reconfiguration and integration of renewable distributed generation for electric vehicles load penetration", *International Journal of Intelligent Engineering & Systems*, Vol. 15, No. 4, pp. 329-338, 2022, doi: 10.22266/ijies2022.0831.30.

[10] S. K. Injeti and V. K. Thunuguntla, "Optimal integration of DGs into radial distribution network in the presence of plug-in electric vehicles to minimize daily active power losses and to improve the voltage profile of the system using bio-inspired optimization algorithms", *Protection and Control of Modern Power Systems*, Vol. 5, pp. 1-5, 2020.

[11] V. Janamala and D. S. Reddy, "Coyote optimization algorithm for optimal allocation of interline–photovoltaic battery storage system in islanded electrical distribution network considering EV load penetration", *Journal of Energy Storage*, Vol. 41, p. 102981, 2021.

[12] D. Chippada and M. D. Reddy, "Optimal planning of electric vehicle charging station along with multiple distributed generator units", *International Journal of Intelligent Systems and Applications*, Vol. 14, pp. 40-53, 2022.

[13] O. Sadeghian, M. N. Heris, M. Abapour, S. S. Taheri, and K. Zare, "Improving reliability of distribution networks using plug-in electric vehicles and demand response", *Journal of Modern Power Systems and Clean Energy*, Vol. 7, No. 5, pp. 1189-1199, 2019.

[14] L. Chen, C. Xu, H. Song, and K. Jermsittiparsert, "Optimal sizing and sitting of EVCS in the distribution system using metaheuristics: A case study", *Energy Reports*, Vol. 7, pp. 208-217, 2021.

[15] A. Mohsenzadeh, S. Pazouki, S. Ardalan, and M. R. Haghifam, "Optimal placing and sizing of parking lots including different levels of charging stations in electric distribution networks", *International Journal of Ambient Energy*, Vol. 39, No. 7, pp. 743-750, 2018.

[16] A. Sadhukhan, S. Sivasubramani, and M. S. Ahmad, "Optimal placement of electric vehicle charging stations in a distribution network", In: *Proc. of 8th International Conference on Power Systems (ICPS) 2019*, Rajasthan, India, pp. 1-6, 2019.

[17] M. Bilal and M. Rizwan, "Integration of electric vehicle charging stations and capacitors in distribution systems with vehicle-to-grid facility", *Energy Sources, Part A: Recovery, Utilization, and Environmental Effects*, pp. 1-30, 2021.

[18] F. Ahmad, A. Iqbal, I. Ashraf, M. Marzband, and I. Khan, "Placement of electric vehicle fast charging stations in distribution network considering power loss, land cost, and electric vehicle population", *Energy Sources, Part A: Recovery, Utilization, and Environmental Effects*, Vol. 44, No. 1, pp. 1693-1709, 2022.

[19] S. M. Alshareef and A Fathy, "Efficient Red Kite Optimization Algorithm for Integrating the Renewable Sources and Electric Vehicle Fast Charging Stations in Radial Distribution Networks", *Mathematics*, Vol. 11, No. 15, p. 3305, 2023.

[20] E. A. Rene, W. S. Fokui, and P. K. Kouonchie, "Optimal allocation of plug-in electric vehicle charging stations in the distribution network with distributed generation", *Green Energy and Intelligent Transportation*, p. 100094. Jun 2 2023

[21] M. Bilal, F. Ahmad, and M. Rizwan, "Techno-economic assessment of grid and renewable

powered electric vehicle charging stations in India using a modified metaheuristic technique", *Energy Conversion and Management*, Vol. 284, p. 116995, May 15 2023.

[22] A. Pal, A. Bhattacharya, A. K. Chakraborty, "Placement of electric vehicle charging station and solar distributed generation in distribution system considering uncertainties", *Scientia Iranica*, Vol. 30, No. 1, pp. 183-206, Feb 1 2023.

[23] M. Mojarad, M. Sedighizadeh, and M. D. Moghadam, "Optimal allocation of intelligent parking lots in distribution system: A robust two-stage optimization model", *IET Electrical Systems in Transportation*, Vol. 12, No. 2, pp. 102-127, 2022.

[24] F. A. Hashim, E. H. Houssein, K. Hussain, M. S. Mabrouk, and W A. Atabany, "Honey Badger Algorithm: New metaheuristic algorithm for solving optimization problems", *Mathematics and Computers in Simulation*, Vol. 192, pp. 84-110, 2022.

[25] S. A. Yasear and H. M. Ghanimi, "A modified honey badger algorithm for solving optimal power flow optimization problem", *International Journal of Intelligent Engineering and Systems*, Vol. 15, No. 4, pp. 142-155, 2022, doi: 10.22266/ijies2022.0831.14.

[26] K. R. Rani, P. S. Rani, N. Chaitanya, and V. Janamala, "Improved bald eagle search for optimal allocation of D-STATCOM in modern electrical distribution networks with emerging loads", *International Journal of Intelligent Engineering and Systems*, Vol. 15, No. 2, pp. 554-563, 2022, doi: 10.22266/ijies2022.0430.49.

[27] V. Janamala and T. K. S. Pandraju, "Static voltage stability of reconfigurable radial distribution system considering voltage dependent load models", *Mathematical Modelling of Engineering Problem*s, Vol. 7, No. 3, pp. 450-458, 2020.